Kerr black hole as a gravitational lens

Igor Bray
Department of Mathematical Physics, University of Adelaide, GPO Box 498, Adelaide, SA 5001, Australia
(Received 24 June 1985)

We present approximate solutions to the equations of motion for a ray of light in the Kerr metric which are correct up to and including second-order terms in $m/r_{\min}$ and $a/r_{\min}$, where m and a are the Kerr mass and spin, respectively, while $r_{\min}$ is the distance of closest approach. We use these expressions to investigate the multi-imaging aspect of the gravitational lens effect.

I. INTRODUCTION

The aim of this paper is to examine the effect that a rotating black hole would have on the appearance of a distant object should it be interposed along the line of sight. A single source has infinitely many images, consisting of the direct rays, i.e., the ones that pass farthest from the black hole and which are therefore least deviated, and the rays which orbit the black hole, once, twice, etc., and then reach the observer. Here we only concern ourselves with the direct images as these are the ones which are most likely to be observed since they are least deformed and hence most intense.[1]

The equations of motion in the Kerr metric were derived by Carter.[2] He did this in the Kerr-Newman coordinate system. These equations have been transformed to Boyer-Lindquist coordinates for simplicity by a number of people including Wilkins[3] and Bardeen.[4] We use Bardeen's version of the equations of motion which are expressed as integrals which can be reduced to elliptic integrals, as our starting point. Unfortunately these prove to be inconvenient to work with and computationally expensive. However, since the direct images have relatively small deviations, we solve these equations up to and including second-order terms in $m/r_{\min}$ and $a/r_{\min}$, where m and a are the Kerr mass and spin, respectively, while $r_{\min}$ is the minimum value of r along the ray's path.

For most astronomical calculations these new equations should suffice as even first-order corrections are difficult enough to observe. The reason that our calculations include second-order terms is that spin comes in only at this order, and our original interest was in the effect of spin. Thus the effect of spin could be observable if the deviation was sufficiently large that the second-order terms give a significant contribution to the first-order terms.

In Sec. II we present and solve the equations of motion up to and including second-order terms in $m/r_{\min}$ and $a/r_{\min}$. In Sec. III we indicate how these expressions may be combined with numerical integration to get excellent results for rays whose paths suffer relatively large deviations. In Sec. IV we use the equations derived in Secs. II and III to investigate the multi-imaging aspect of the gravitational lens effect due to a rotating black hole.

II. SOLVING THE EQUATIONS OF MOTION

The form of the Kerr metrics in the Boyer-Lindquist coordinates is given by

$$ds^2=\frac{\rho^2}{\Delta}dr^2+\rho^2 d\theta^2+\frac{\sin^2\theta}{\rho^2}[a\,dt-(r^2+a^2)d\phi]^2 - \frac{\Delta}{\rho^2}(dt-a\sin^2\theta\, d\phi)^2 , \tag{1}$$

where

$$\rho^2=r^2+a^2\cos^2\theta$$

and

$$\Delta=r^2-2mr+a^2 .$$

The constants m and a are, respectively, the mass and spin parameters of the Kerr metric with $m=|m|\geq|a|$.

The equations of motion for a ray of light in the Boyer-Lindquist coordinates (r,θ,ϕ,t) are

$$\int^r\frac{dr}{\pm[R(r)]^{1/2}}=\int^\theta\frac{d\theta}{\pm[\Theta(\theta)]^{1/2}} , \tag{2}$$

$$\phi=\int^r\frac{r^2\lambda+2mr(a-\lambda)}{\pm\Delta[R(r)]^{1/2}}dr+\int^\theta\frac{\lambda\cot^2\theta}{\pm[\Theta(\theta)]^{1/2}}d\theta , \tag{3}$$

and

$$t=\int^r\frac{r^2(r^2+a^2)+2amr(a-\lambda)}{\pm\Delta[R(r)]^2}dr + \int^\theta\frac{a^2\cos^2\theta}{\pm[\Theta(\theta)]^{1/2}}d\theta , \tag{4}$$

where

$$R(r)=r[r(r^2+a^2)+2a^2m]-4amr\lambda -(r^2-2mr)\lambda^2-\Delta\eta \tag{5}$$

and

$$\Theta(\theta)=\eta+a^2\cos^2\theta-\lambda^2\cot^2\theta . \tag{6}$$

The parameters λ and η are constants of the motion which will be discussed later. The integrals are along the path of motion.

Suppose a ray of light originates at the source with coordinates $(r_s,\theta_s,\phi_s,t_s)$, passes by the black hole and arrives at the observer's coordinates $(r_o,\theta_o,\phi_o,t_o)$. Along this path the r coordinate ranges from r_s to $r_{\min}$, to r_o, while θ ranges from θ_s to $\theta_{\min}$ or $\theta_{\max}$ through to θ_o. These are relevant integral paths. The sign of $[R(r)]^{1/2}$ is

 ©1986 The American Physical Society

chosen to be positive if we are integrating from $r_{\min}$ to r_o and negative otherwise. Similarly the sign of $[\Theta(\theta)]^{1/2}$ is taken to be positive if integrating from $\theta_{\min}$ to θ_s or θ_o and negative otherwise.

For large r, (r,θ,ϕ) can be thought of as spherical polar coordinates. Converting these rectangular coordinates in the usual way, define the observer to be at $(r_o\sin\theta_o,0,r_o\cos\theta_o)$, i.e., set $\phi_o=0$. Defining the tangent to the ray at the observer to intersect the plane $x=0$ at the point $(0,\alpha_i,\beta_i/\sin\theta_o)$, it can be shown that

$$\alpha_i=-\frac{r_o^2\sin^2\theta_o\dot{\phi}_o}{\sin\theta_o+r_o\cos\theta_o\dot{\theta}_o} \tag{7}$$

and

$$\frac{\beta_i}{\sin\theta_o}=\frac{r_o^2\dot{\theta}_o}{\sin\theta_o+r_o\cos\theta_o\dot{\theta}_o}\ . \tag{8}$$

Here $\dot{\theta}_o$ means $(d\theta/dr)\,|_{r=r_o}$ and $\dot{\phi}_o$ means $(d\phi/dr)\,|_{r=r_o}$. Therefore with the aid of Eqs. (2) and (3)

$$\alpha_i\approx\frac{\lambda}{\sin\theta_o\left[1-\dfrac{\lambda^2+\eta}{r_o^2}\right]^{1/2}\mp\cos\theta_o\dfrac{[\Theta(\theta_o)]^{1/2}}{r_o}} \tag{9}$$

and

$$\frac{\beta_i}{\sin\theta_o}\approx\pm\frac{[\Theta(\theta_o)]^{1/2}}{\sin\theta_o\left[1-\dfrac{\lambda^2+\eta}{r_o^2}\right]^{1/2}\mp\cos\theta_o\dfrac{[\Theta(\theta_o)]^{1/2}}{r_o}}\ . \tag{10}$$

By definition α_i and β_i are the coordinates of the position of the image projected along the tangent to the ray at the observer onto the plane through the black hole and normal to the line connecting it with the observer (see Fig. 1). They are observable quantities and are related to the constants of the motion λ and η, as can be seen from Eqs. (9) and (10). In fact we can rearrange Eqs. (9) and (10) to get λ and η as functions of α_i and β_i. We find that

$$\lambda\approx\frac{-r_o\sin\theta_o\alpha_i}{[\beta_i^2+\alpha_i^2+(r_o-\beta_i\cot\theta_o)^2]^{1/2}} \tag{11}$$

and

$$\sqrt{\eta}\approx\frac{\mp r_o(\beta_i^2+\alpha_i^2\cos^2\theta_o)^{1/2}}{[\beta_i^2+\alpha_i^2+(r_o-\beta_i\cot\theta_o)^2]^{1/2}}\ , \tag{12}$$

where the $\mp$ sign is the sign of $\dot{\theta}_o$ and the approximation excludes first and higher orders in $mr_{\min}^2/r_o^3$. The minimum value of r is determined by $R(r)$. Since our rays are not captured by the black hole, $R(r)$ has four real roots, the largest of which is $r_{\min}$. Since for $\theta_o=\pi/2$ and large r_o, $\alpha_i\approx-\lambda$ and $\beta_i\approx\pm\sqrt{\eta}$, we expect for small deflections, $r_{\min}$ to be of order $(\lambda^2+\eta)^{1/2}$. Thus, we solve for $r_{\min}$ by supposing that

$$r_{\min}\approx(\lambda^2+\eta)^{1/2}\left[1+\sum_j c_jx_j\right],$$

where x_j are the first- or second-order terms in $m/(\lambda^2+\eta)^{1/2}$ or $a/(\lambda^2+\eta)^{1/2}$ c_j are real numbers, and the summation is over all possible first- and second-order terms. To obtain the coefficients, we evaluate $R(r_{\min})$, drop third- and higher-order terms, and then set the result to zero to find that

$$r_{\min}\approx(\lambda^2+\eta)^{1/2}\left[1-\frac{m}{(\lambda^2+\eta)^{1/2}}-\frac{3m^2}{2(\lambda^2+\eta)}-\frac{a^2}{2(\lambda^2+\eta)}+\frac{a^2\eta}{2(\lambda^2+\eta)^2}+\frac{2am\lambda}{(\lambda^2+\eta)^{3/2}}\right]. \tag{13}$$

Since we are interested in the gravitational lens effects of a black hole which has been interposed somewhere in between us and a distant luminous object, we have that $R(r)\approx r^4$ for $r=r_s$ and $r=r_o$. From Eq. (13) onward $\approx$ will be taken to mean $=$ up to and including second-order terms in $m/(\lambda^2+\eta)^{1/2}$ and $a/(\lambda^2+\eta)^{1/2}$, as well as, where relevant, first- and second-order terms in $r_{\min}/r_s$ and $r_{\min}/r_o$.

From a computational viewpoint it is important to keep track of the contributions to the integrals by the $r_{\min}/r_s$ and $r_{\min}/r_o$ terms. These contributions become redundant if they are less than the third-order terms in $m/(\lambda^2+\eta)^{1/2}$ and $a/(\lambda^2+\eta)^{1/2}$, which is more probable from a physical point of view. On the other hand, it is useful to leave them in, so that we can check our expressions in the limit as m, and therefore a, goes to zero.

Substituting (13) back into (5) we find that $R(r_{\min})\approx 0$. For the extreme Kerr black hole, $a=m$, it is interesting to note that in the special case where the ray of light stays in the equatorial plane, $\beta_i=\eta=0$, and with $\lambda=|\lambda|$, that $r_{\min}=\lambda-m$ is indeed the exact solution for the distance of closest approach, i.e., $R(\lambda-m)=0$. This is surprising as no such simple solutions for $r_{\min}$ exist in the Schwarzschild case.

Now we are in a position to evaluate the left-hand side of (2). With the above assumptions we have

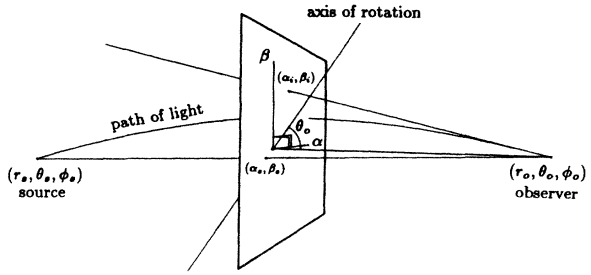

FIG. 1. The polar coordinates (r,θ,ϕ) are defined by the axis of rotation. The α-β plane is perpendicular to the line passing through (0,0)—the position of the black hole, and the observer. Point (α_i,β_i) is the observed position of an image of the source, while (α_s,β_s) is the projected position of the source onto the α-β plane along the line through the source and the observer. It can be shown that $\lim_{m\to 0}(\alpha_i\beta_i)=(\alpha_s,\beta_s)$. All projections are carried out in the absence of the mass.

$$\int^{r}\frac{dr}{\pm[R(r)]^{1/2}}\approx 2\int_{r_{\min}}^{\infty}\frac{dr}{[R(r)]^{1/2}}-\frac{r_s+r_o}{r_s r_o}\,.$$

Defining $x=r_{\min}/r$, $f(x)=\eta(1+x^2)/(\lambda^2+\eta-a^2)$, and $g(x)=-2\left[\frac{(\lambda-a)^2+\eta}{\lambda^2+\eta-a^2}\right]\left[\frac{x^2+x+1}{x+1}\right]$, we have

$$2\int_{r_{\min}}^{\infty}\frac{dr}{[R(r)]^{1/2}}=\frac{2}{(\lambda^2+\eta-a^2)^{1/2}}\int_0^1\frac{dx}{\left[(1-x^2)\left[1+\frac{a^2}{r_{\min}^{\,2}}f(x)+\frac{m}{r_{\min}}g(x)\right]\right]^{1/2}}$$

$$\approx\frac{2}{(\lambda^2+\eta-a^2)^{1/2}}\int_0^1\frac{dx}{(1-x^2)^{1/2}}\left[1-\frac{a^2}{2r_{\min}^{\,2}}f(x)-\frac{m}{2r_{\min}}g(x)+\frac{3m^2}{8r_{\min}^{\,2}}g^2(x)\right].$$

So by evaluating this integral

$$\int^{r}\frac{dr}{\pm[R(r)]^{1/2}}\approx\frac{1}{(\lambda^2+\eta-a^2)^{1/2}}\left[\pi\left[1-\frac{3a^2\eta}{4(\lambda^2+\eta)^2}+\frac{15m^2}{4(\lambda^2+\eta)}\right]+\frac{4m}{(\lambda^2+\eta)^{1/2}}-\frac{8ma\lambda}{(\lambda^2+\eta)^{3/2}}\right]-\frac{r_s+r_o}{r_s r_o}\,. \tag{14}$$

Next, we need to find the maximum or the minimum value that θ takes along the ray's path. This we find by solving $\Theta(\theta)=0$. We find that

$$\cos\theta_{\min/\max}\approx\pm\left[\frac{\eta}{\lambda^2+\eta}\right]^{1/2}\left[1+\frac{a^2\lambda^2}{2(\lambda^2+\eta)^2}\right], \tag{15}$$

where the positive sign corresponds to $\cos\theta_{\min}$ and the negative sign corresponds to $\cos\theta_{\max}$. Since $\dot{\theta}_o=\pm[\Theta(\theta_o)]^{1/2}/[R(r_o)]^{1/2}$ Eq. (10) implies, for sufficiently large r_o or $\theta_o=\pi/2$, that the sign of β_i determines whether θ attained $\theta_{\min}$ or $\theta_{\max}$. If β_i is negative then θ must have reached $\theta_{\max}$, otherwise, $\theta_{\min}$. Evaluating the right-hand side of (2) we find that

$$\int^{\theta}\frac{d\theta}{\pm[\Theta(\theta)]^{1/2}}\approx\frac{1}{(\lambda^2+\eta-a^2)^{1/2}}\left[1+\frac{a^2\lambda^2}{2(\lambda^2+\eta)^2}\right]\int^{\sigma}\frac{d\sigma}{1+\frac{a^2\eta}{2(\lambda^2+\eta)^2}\cos^2\sigma}$$

$$\approx\frac{1}{(\lambda^2+\eta-a^2)^{1/2}}\left[1-\frac{3a^2\eta}{4(\lambda^2+\eta)^2}\right]\left\{\pi\pm\arctan\left[\left[1+\frac{a^2\eta}{4(\lambda^2+\eta)^2}\right]\cot\sigma_s\right]\right.$$

$$\left.\pm\arctan\left[\left[1+\frac{a^2\eta}{4(\lambda^2+\eta)^2}\right]\cot\sigma_o\right]\right\}, \tag{16}$$

where σ is defined by

$$\cos\theta=\left[\frac{\eta}{\lambda^2+\eta}\right]^{1/2}\left[1+\frac{a^2\lambda^2}{2(\lambda^2+\eta)^2}\right]\cos\sigma\,, \tag{17}$$

and where the positive sign corresponds to the path where θ attained $\theta_{\max}$, and the negative sign corresponds to the path where θ attained $\theta_{\min}$.

Equating (14) and (16), and using (17) we find that

$$\cos\theta_s\approx-\cos\theta_o\cos\delta\pm\sin\delta\left[\frac{\eta}{\lambda^2+\eta}-\cos^2\theta_o\right]^{1/2}, \tag{18}$$

where

$$\delta=\frac{15\pi}{4}\frac{m^2}{\lambda^2+\eta}+\frac{4m}{(\lambda^2+\eta)^{1/2}}-\frac{8ma\lambda}{(\lambda^2+\eta)^{3/2}}-(\lambda^2+\eta)^{1/2}\frac{r_s+r_o}{r_s r_o}\,. \tag{19}$$

The above equation is correct provided that θ_o is not too close to $\theta_{\min}$ or $\theta_{\max}$, in particular, we must have that $\sigma_o\in[\,|\delta|,\pi-|\delta|\,]$. This ensures that the ray takes the $\theta_s\to\theta_{\min/\max}\to\theta_o$ path, assumed above, as opposed to say the

$\theta_s \to \theta_{\min/\max} \to \theta_{\max/\min} \to \theta_o$ or $\theta_s \to \theta_o$ paths.

Now we consider the ϕ integral. Equation (3), with the assistance of (2), can be rewritten as

$$\phi=\phi_o-\phi_s=\int^r \frac{a(2mr-a\lambda)}{\pm\Delta[R(r)]^{1/2}}dr+\int^\theta \frac{\lambda\, d\theta}{\pm\sin^2\theta[\Theta(\theta)]^{1/2}} . \tag{20}$$

With a considerable amount of effort using methods employed above, it can be shown from evaluation of Eq. (20) that

$$\phi_o-\phi_s\approx\pi\frac{\lambda}{|\lambda|}+\frac{4ma}{\lambda^2+\eta}+\frac{\lambda\delta\csc^2\theta_o}{(\lambda^2+\eta)^{1/2}}\left[1\mp\delta\cot\theta_o\csc\theta_o\left[\frac{\eta}{\lambda^2+\eta}-\cos^2\theta_o\right]^{1/2}\right], \tag{21}$$

where δ is defined as above. Here it is the negative sign that corresponds to the path where θ attained $\theta_{\max}$ and the positive sign for the $\theta_{\min}$ path.

Finally we solve Eq. (4). Since the greatest contribution that the integral involving θ can make is of second order, it turns out that this contribution is independent of whether θ attained $\theta_{\min}$ or $\theta_{\max}$, and even θ_o. In particular using the same transformations as in the evaluation of the right-hand side of Eq. (2), it can be shown that

$$\int^\theta \frac{a^2\cos^2\theta}{\pm[\Theta(\theta)]^{1/2}}d\theta\approx\frac{\pi}{2}\frac{\eta a^2}{(\lambda^2+\eta)^{3/2}} . \tag{22}$$

To solve the integral involving r in Eq. (4) we use the same transformations that we used to solve the left-hand side of Eq. (2), to get

$$\int_{r_{\min}}^{r_s}\frac{r^2(r^2+a^2)+2amr(a-\lambda)}{\Delta[R(r)]^{1/2}}dr\approx r_s-\frac{r_{\min}^2}{2r_s}-\frac{4am\lambda}{r_{\min}^2}+2m\ln\left[\frac{2r_s}{r_{\min}}\right]+\frac{\pi}{2}\left[\frac{15m^2}{2r_{\min}}-\frac{a^2\eta}{2r_{\min}^3}\right]+m\left[1-\frac{2m}{r_{\min}}-\frac{r_{\min}}{r_s}\right].$$

Therefore adding the integral from $r_{\min}$ to r_o as well as Eq. (22), we find that

$$t\approx r_s+r_o-\frac{r_{\min}^2}{2}\left[\frac{1}{r_s}+\frac{1}{r_o}\right]-\frac{8am\lambda}{r_{\min}^2}+2m\ln\left[\frac{4r_sr_o}{r_{\min}^2}\right]+\frac{15\pi m^2}{2r_{\min}}+2m\left[1-\frac{2m}{r_{\min}}-\frac{r_{\min}}{2}\left[\frac{1}{r_s}+\frac{1}{r_o}\right]\right] . \tag{23}$$

III. LARGE DEVIATIONS

From past experience with Schwarzschild black holes we know that the deviation of a ray of light is small whenever the ratio $m/r_{\min}$ is small. In the Kerr case this is still true; however, a new factor plays an important part in the size of the deviation. Now the sign of λ as well as $m/r_{\min}$ determines the size of the deviation. This is most evident in the equatorial plane as the effect of spin is most apparent there. Assuming that $a=|a|$, a positive λ corresponds to a ray traveling with the spin, which is therefore not as greatly deviated as the ray with negative λ, which corresponds to a ray traveling against the spin. As a result, we find that the accuracy of our approximations in the previous section depends on the sign of λ. This is easily seen when substituting the approximate value for $r_{\min}$ into $R(r)$. We find that $R(r_{\min})$ is much closer to 0 for positive λ than for negative λ. Similarly, any of the integrals approximated above which have terms proportional to λ are more accurate for positive λ than for negative λ. Fortunately the integrals involving θ have λ appear as λ^2 only, and furthermore, have higher-order terms with integral powers of $a^2/(\lambda^2+\eta)$. Thus the approximations of these integrals remain good for relatively high ratios of $m/r_{\min}$ and are independent of the sign of λ.

There is another more significant source of error which comes in the evaluation of δ. The value δ is obtained by equating Eqs. (14) and (16) and setting δ to be equal to the sum of the arctangents. When these equations were equated we saw that the "large" $\pi/(\lambda^2+\eta-a^2)^{1/2}$ terms canceled on both sides leaving us with a small result for δ. Since the absolute error of Eq. (14) is of third order and is particularly large for negative λ, the relative error in δ can easily become unacceptable. If this occurs then Eq. (14) should be evaluated numerically, something which can be done quickly using Gauss-Jacobi quadratures and even quicker using the method of Elhay and Kautsky,[5] where successive approximations use nodes already used in previous approximations. Thus the new δ becomes the numerical integral minus the term proportional to π of Eq. (16), and then Eq. (18) may still be used to give remarkably good results.

In the evaluation of ϕ_s, the integral containing r may give poor results for negative λ. In this event evaluate the integral numerically, add the result to Eq. (21) and replace the $4ma/(\lambda^2+\eta)$ term by $(\pi/2)a^2\lambda/(\lambda^2+\eta)^{3/2}$.

Another advantage of this technique is that we are no longer limited to large values of r_s and r_o as these are absorbed in the numerical evaluation.

IV. NUMERICAL INVESTIGATION

We assume that our black hole is an extreme Kerr black hole, i.e., $|a|=m$. Without any loss of generality we choose $a=m$ and $\phi_o=0$. The choice of θ_o is not arbitrary. For simplicity and maximal effect of spin we take $\theta_o=\pi/2$. Equations (18) and (21) now become

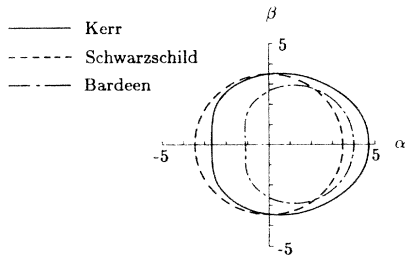

FIG. 2. Regions in which (α_i,β_i) correspond to sources whose rays suffer "large" deviations. Bardeen's region is calculated by setting $R(r)=\dot{R}(r)=0$.

$$\cos\theta_s \approx \pm\sin\delta\left[\frac{\eta}{\lambda^2+\eta}\right]^{1/2} \tag{24}$$

and

$$-\phi_s \approx \pi\frac{\lambda}{|\lambda|}+\frac{4m^2}{\lambda^2+\eta}+\frac{\lambda\delta}{(\lambda^2+\eta)^{1/2}}\ , \tag{25}$$

where

$$\delta=\frac{15\pi}{4}\frac{m^2}{\lambda^2+\eta}+\frac{4m}{(\lambda^2+\eta)^{1/2}}-\frac{8m^2\lambda}{(\lambda^2+\eta)^{3/2}} -(\lambda^2+\eta)^{1/2}\frac{r_s+r_o}{r_s r_o}\ . \tag{26}$$

We next need to choose r_s, r_o, and m.

As stated earlier we are mainly interested in the effect of spin. Since spin appears only at second order we require relatively large deflections. However, we project the position of the source and the image onto the same plane. So that the sources and their images will not be too far apart we choose a relatively small value for r_o. We also take $r_s=r_o$, as the deflection is maximal if the deflecting object is between the source and the observer. The following diagrams (cf. Bray[6]) were generated by choosing $m=a=\frac{1}{2}$ and $r_o=r_s=14$.

Having chosen all the necessary parameters we proceed as follows. The plane of Fig. 1, which is parametrized by α and β, is considered as a fine grid. Each point of the grid is a possible position of an image. This point (α_i,β_i) is used to define λ and η via Eqs. (11) and (12). These are then put into Eqs. (24) and (25) which yield θ_s and ϕ_s. The position of the source is projected onto this plane

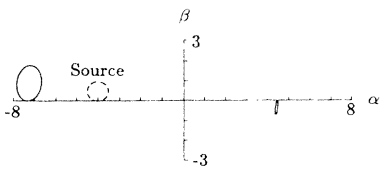

FIG. 3. Images of a source near the boundary of the Kerr region of Fig. 4. Note that the image on the left-hand side, which corresponds to rays with small deviations, is amplified. On the other hand, the image on the right-hand side, which corresponds to rays with large deviations, is diminished, and therefore is less likely to be observed.

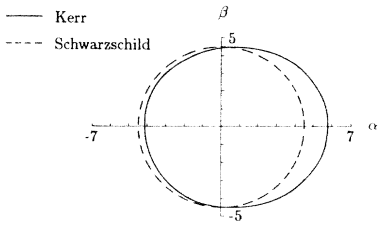

FIG. 4. Sources within these regions have two observable images, those not within these regions have only one.

along the line through the source and the observer, see Fig. 1. Thus

$$\alpha_s=\frac{r_s r_o\sin\theta_s\sin\phi_s}{r_o-r_s\cos\phi_s\sin\theta_s} \tag{27}$$

and

$$\beta_s=\frac{r_s r_o\cos\theta_s}{r_o-r_s\cos\phi_s\sin\theta_s}\ . \tag{28}$$

It is not difficult to show that in the limit as $m\to 0$ the source position and its image positions are the same, as expected.

This calculation is done for every point of the grid which is not "too far away" from the central point (0,0). In particular, the following diagrams were generated with $||(\alpha_i,\beta_i)||\leq 10$.

Points (α_i,β_i) in the neighborhood of (0,0) correspond to rays which suffer "large" deflections. These calculations were done using the numerical integration technique described in Sec. III. In the diagrams we defined a ray to have a large deflection if either $||(\alpha_i,\beta_i)-(\alpha_s,\beta_s)||\geq 8$, or if the angle θ does not vary as $\theta_s\to\theta_{\min/\max}\to\theta_o$. The latter condition assigns large deflections to rays which orbit the black hole or are captured by the black hole. Figure 2 shows the regions in which the rays suffer large deviations for both the Kerr and Schwarzschild black holes. The Kerr region is comparable with the region due to the black hole being illuminated by an extended light source whose angular size is larger than that of the black hole (see Bardeen[4]).

A point (α_i,β_i) is considered to be an observable image of a source if the ray did not suffer a large deflection. This definition of an observable image is borne out by Fig. 3, where the image corresponding to rays with large deflections is quite small and therefore is less likely to be observed. Figure 4 shows the distribution of the number of observable images as a function of the position of the source. For contrast we compare the results for the Kerr black hole with those for the Schwarzschild black hole.

ACKNOWLEDGMENTS

The author wishes to thank P. Szekeres for some valuable discussions, as well as S. Elhay for his assistance with numerical integration techniques. The author is also grateful to the Computing Centre of the University of Adelaide for the use of their facilities.

[1]C. T. Cunningham and J. M. Bardeen, Astrophys. J. **183**, 237 (1973).
[2]B. Carter, Phys. Rev. **174**, 1559 (1968).
[3]D. C. Wilkins, Phys. Rev. D **5**, 814 (1972).
[4]J. M. Bardeen, in *Black Holes,* edited by C. DeWitt and B. S. DeWitt (Gordon and Breach, New York, 1973).
[5]S. Elhay and J. Kautsky, Aust. Comput. Sci. Commun. **6**, 15-1 (1984).
[6]I. Bray, Mon. Not. R. Astron. Soc. **208**, 511 (1984).